International Journal of Heat and Mass Transfer 52 (2009) 497–503

Contents lists available at ScienceDirect

International Journal of Heat and Mass Transfer

journal homepage: www.elsevier.com/locate/ijhmt

# Analytical solution of the laser-induced temperature distribution across internal material interfaces

Klaus Zimmer *

*Leibniz-Institute of Surface Modification, Department of Ion Beam Technology, Permoserstraße 15, 04318 Leipzig, Germany*

ARTICLE INFO

*Article history:*
Received 13 October 2006
Received in revised form 13 February 2008
Available online 31 August 2008

*Keywords:*
Analytical solution
Temperature distribution
Laser
Heating
Solid–liquid interface

ABSTRACT

The paper presents an analytical solution of the heat conduction equation with constant coefficients for laser irradiation at the interface of two materials by applying Laplace transformation. Special attention is put on liquid–solid interfaces. The model considers the laser absorption in only one material as well as at the interface. The temperature distribution and the thermal flow across the materials interface as well as the energy efficiency to heat the solid material were studied in dependence on selected material properties, the laser beam absorption, and the length of the laser pulse. High solid surface temperatures can be achieved with high absorption liquids, sufficient interface absorption, and at short laser pulses. The comparison with numerical results shows a good congruence.



## 1. Introduction

The interaction of laser radiation with matter is of great interest for a lot of industrial applications due to the advantages of laser processing techniques such as localized interaction, low overall material alteration, 3D-capabilities, force-free processing, etc. Laser-matter interaction processes are very important for biological and medical purposes in which liquid phases often are involved. Often, the main process of laser-matter interaction is the heat generation due to the laser energy absorption into the material. Bäuerle [1] summarizes the processes upon laser irradiation of materials and presents different solutions of the heat transfer problem for different irradiation configurations. A general introduction of solving the heat transfer equation together with a broad range of different solutions for different heat conduction problems and applications is given by Carslaw and Jaeger [2].

The predominant number of industrial laser applications makes use of the thermal effect of laser irradiation of solid materials. Therefore, many technical and scientific papers dealt with the thermal effects of laser beam absorption. Because typically absorbing solids are used in laser processing the heat conduction equation is solved especially for semi-infinite substrates often without heat losses across the surface [1].

Further, different laser pulse shapes and energy density distributions have been considered in solving the heat equation. Sometimes phase transitions, layered substrates, and chemical reactions were included in the investigation [1]. In addition, laser-induced melting processes are studied for different materials and conditions due to the technical importance [3]. Even if the laser pulse length is shorter than the electron–phonon coupling time and nonlinear interaction mechanisms happen, which can be expected for ultra-short laser pulses, thermal processes have to be considered after thermalization of the absorbed laser energy [4,5]. For a more detailed description of the energy dissipation of ultra-short laser pulses ($t_p < 10^{-11}$ s), Anisimov et al. proposed a two-temperature model that includes the energy transport by the electron and the phonon system and the coupling of both systems by relaxations terms [6]. This and similar approaches [5] have been used to model laser-matter interaction processes. For time scales larger than the electron–phonon relaxation time (typical $t \sim 10^{-11}$–$10^{-12}$ s), the two-temperature model merges into the ordinary heat conduction equation.

The modeling of laser-induced processes allows not only the estimation of experimental parameters but also helps to understand the laser-matter interaction and the material processing procedure in general. Due to the complexity of current problems of laser materials heating an increasing number of numerical techniques is used for solving such problems [7,8]. Nevertheless, analytical solutions offer a fast access to the principal behavior of the system under consideration even if approximations (constant coefficients, simple temporal laser pulse shape, etc.) limit the validity for the real application.

Currently, an increasing number of technical, biological, and medical laser applications is accomplished at the solid–liquid interface [9]. For example, laser ablation in liquids [10–13], laser-induced wet etching processes (LIBWE) [1,14,15], or steam cleaning [16] are well known. Especially laser-induced backside wet

* Tel.: +49 (0)341 235 3287; fax: +49 (0)341 235 2584.
*E-mail address:* klaus.zimmer@iom-leipzig.de

0017-9310/$ - see front matter © 2008 Elsevier Ltd. All rights reserved.
doi:10.1016/j.ijheatmasstransfer.2008.03.034

**Nomenclature**

*Symbols*

| | |
|---|---|
| $A$ | coefficient of heat flow across the interface (W m$^{-2}$) |
| $c_p$ | specific heat (J kg$^{-1}$ K$^{-1}$) |
| $D$ | thermal diffusivity (m$^2$ s$^{-1}$) |
| $F$ | laser fluence $F = I_L t_p$ (J m$^{-2}$) |
| $I_L$ | power density of the laser beam (W m$^{-2}$) |
| $J$ | heat flux (W m$^{-2}$) |
| $k$ | thermal conductivity (W m$^{-1}$ K$^{-1}$) |
| $L_T$ | thermal diffusion length (m) |
| $L_O$ | optical penetration depth (m) |
| $s$ | Laplace variable |
| $S$ | laser-induced heat generation |
| $t$ | time (s) |
| $t_p$ | pulse duration (s) |
| $T$ | temperature (K) |
| $T_0$ | ambient temperature (K) |
| $V$ | temperature in the Laplace domain (K) |
| $x$ | spatial variable (m) |

*Greek symbols*

| | |
|---|---|
| $\alpha$ | absorption coefficient (m$^{-1}$) |
| $\lambda$ | wavelength (m) |
| $\rho$ | density (kg m$^{-3}$) |

*Subscripts*

| | |
|---|---|
| L | liquid |
| I | solid–liquid interface |
| S | solid |
| V | volumetric |
| 1 | region 1, e.g. the solid |
| 2 | region 2, e.g. the liquid |

*Abbreviations*

| | |
|---|---|
| LIBWE | laser-induced backside wet etching |
| n.s. | not specified |

etching processes [17] make use of a laser-heated absorbing liquid; first numerical investigations of the laser etching process were carried out [18] but show, that the solely laser-induced heating of the liquid is not able to exceed the melting temperature at the etch threshold. To the best of my knowledge a specific solution of the heat conduction equation for laser irradiation of an internal solid–liquid material interface as depicted in Fig. 1 is not available.

In the solution of the heat conduction equation the heat flow across the interface has to be considered additionally. This heat conduction causes the heating of the non-absorbing material, e.g. the solid, and the cooling of the absorbing material, e.g. the liquid, respectively.

## 2. Model for laser heating of a solid–liquid interface

A lot of former work solving the heat conduction equation at material interfaces or surfaces concentrates on long-time processes. Hence, heat transfer by convection or radiation was considered in the solutions. However, current laser techniques are able to provide energetic laser pulses on the ns or even the fs/ps time scale. Due to the short-time scale of the laser pulse the thermal flow across interfaces or surfaces due to convection and even thermal radiation can be neglected in comparison to the energy flux of the heating laser beam for temperature calculation during the pulse duration.

For irradiation of the internal interface of adjacent or adjoining materials by laser radiation, one material must be transparent at the applied wavelength. The other material must show a sufficient absorption in order to ensure the intended interaction of the laser beam with the materials.

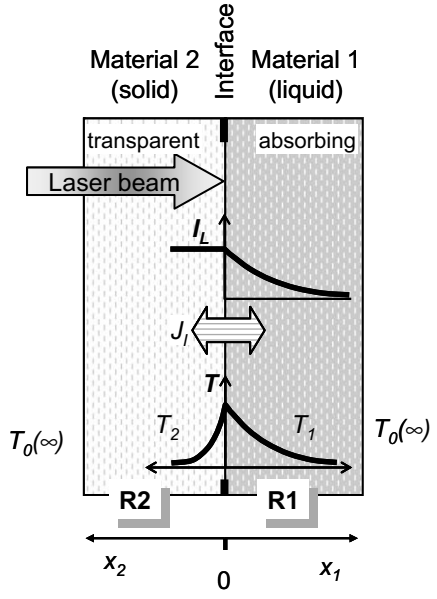


**Fig. 1.** Sketch of laser heating of a solid–liquid interface. The laser absorption ($I_L$), the temperature distribution ($T$) in both materials, and the heat conduction ($J_I$) across the interface are shown additionally.

### 2.1. Set-up of the model for laser heating

In setting up the problem, constant material coefficients are presumed. The whole problem is considered to be one-dimensional although it is clear that a three-dimensional heat flow occurs in general. However, for large spot size irradiation (beam size $\gg$ characteristic lengths) a one-dimensional approximation is valid.

For the above specified problem the one-dimensional heat conduction equation with constant coefficients can be written as follows:

$$\frac{\partial^2 T}{\partial x^2} - \frac{1}{D}\cdot\frac{\partial T}{\partial t} = \frac{1}{k} S(x,t), \tag{1}$$

where $T$ is the excess temperature with respect to the ambient temperature $T_0$.

The confinement of the thermal processes upon direct laser heating of a solid surface is determined by some characteristic lengths that can be either the laser penetration depth or the thermal diffusion length given by $L_O = \alpha^{-1}$ and $L_T = 2\cdot\sqrt{D_T\cdot t}$ with $D_T = k/\rho\cdot c_p$, respectively. Depending on these characteristic lengths the heat distribution in single materials is often called optically or thermally confined. However, due to different materials of the interface the parameters of both materials can cause different confinements in both material regions. Considering typical material properties of absorbing liquids and transparent solids, see Table 1, the thermal processes are often optically confined in the absorbing material and thermally confined in the transparent material. In some cases, for example using a highly absorbing liquid (e.g. metals [19]), an interface absorption of the laser radiation can be assumed. This problem of interface heating has been solved already by Carslaw and Jaeger [2]. For $L_T \gg L_O$ the tempera-

**Table 1**
Thermophysical and optical properties of selected solids and liquids and chosen "standard" material properties

| Properties ($T \sim 300$ K) | By default for the liquid | Acetone [22] | Toluene [22] | By default for the solid | Fused silica [22] | Sapphire [23] |
|---|---|---|---|---|---|---|
| Density (kg m$^{-3}$) | 1000 | 784.6 | 858 | 2500 | 2202 | 3980 |
| Specific heat capacity (J kg$^{-1}$ K$^{-1}$) | 2000 | 2176 | 1705 | 700 | 750 | 761 |
| Thermal conductivity (W m$^{-1}$ K$^{-1}$) | 0.2 | 0.18 | 0.134 | 2 | 1.36 | 25.2[a] |
| Absorption coefficient ($\lambda$ = 248 nm) (m$^{-1}$) | $10^6$ | n.s. | $2.08 \times 10^5$ | 0 | $<10^{-3}$ | $<10^{-2}$ |

[a] Perpendicular to optical axis.

ture for finite optical absorption lengths can be approximated well by interface absorption solutions. With the given default material properties the condition $L_T \gg L_O$ is fulfilled for $t > 100$ μs.

The problem of laser-heating of an internal surface is depicted in Fig. 1 together with the most relevant processes using the example of a solid–liquid interface.

Both the liquid and the solid regions are semi-infinite. It is assumed that region 2 (e.g. the solid) is transparent and the laser radiation is absorbed only in the material region 1 (e.g. the liquid) or at the interface of both. In particular, the interface with its specific properties, e.g. an increased absorption due to the higher defect density, was taken into account. The reflection of the laser beam is neglected but can easily be included into the solution. Heat transfer by radiation is not regarded and the convection of the liquid is neglected, too. Both assumptions usually are valid for short-pulse laser irradiation. Materials decomposition or etching as well as plasma formation are disregarded although they are typical processes at high-power laser irradiation of solid surfaces and material processing.

The heating cycle is the most important time scale in applications of pulsed laser processing because the highest temperature and therefore the strongest impact to the material can be expected within the pulse length. However, the cooling cycle is also of relevance as the average thermal load is given by both the heating and the cooling cycle and further on secondary, thermally stimulated processes might run at the cooling cycle that have influence on the overall laser-matter interaction during prolonged laser irradiation.

As the indirect heating of a transparent solid material immersed into an absorbing liquid is a required solution for practical applications further considerations concentrate on this particular case. The materials for the calculations are chosen according to technical relevance.

### 2.2. Analytical solution for laser heating of the solid–liquid interface

For the above-mentioned problem the partial differential equation of heat conduction can be separated in two equations for each material region: R1 – the absorbing material (liquid) – and R2 – the transparent material (solid)

$$\mathrm{R1}: \quad \frac{\partial^2 T_1}{\partial x_1^2} - \frac{1}{D_1}\cdot\frac{\partial T_1}{\partial t} = \frac{1}{k_1} S(x_1,t) \quad 0 \leqslant x_1 \leqslant \infty, \tag{2}$$

$$\mathrm{R2}: \quad \frac{\partial^2 T_2}{\partial x_2^2} - \frac{1}{D_2}\cdot\frac{\partial T_2}{\partial t} = 0 \quad 0 \leqslant x_2 \leqslant \infty, \tag{3}$$

where $D$ is the thermal diffusivity and $S$ is the term of heat generation by the laser absorption.

The initial and boundary conditions are defined by

$$T_1(x_1,0) = T_2(x_2,0) = 0 \qquad 0 \leqslant x_{1,2} \leqslant \infty, \quad t = 0 \tag{4}$$

and

$$T_1(\infty,t) = T_2(\infty,t) = 0 \qquad x_{1,2} \to \infty, \quad 0 \leqslant t \leqslant \infty. \tag{5}$$

At the materials interface the boundary condition is

$$k_1 \cdot \frac{\partial T_1(0,t)}{\partial x_1} = k_2 \cdot \frac{\partial T_2(0,t)}{\partial x_2} = |J_I| \tag{6}$$

for sole volume absorption. Supposing linear absorption of the laser radiation in the material region 1 the source term in Eq. (2) is equivalent to

$$S(x_1,t) = I_V \cdot \alpha_1 \cdot \mathrm{e}^{-\alpha_1 \cdot x_1} \qquad 0 \leqslant x_1 \leqslant \infty, \quad 0 \leqslant t \leqslant t_p \tag{7}$$

according to Beer's law, where $I_V$ is the laser power density at the interface, which is assumed to be constant, $t_p$ is the irradiation time, e.g. the length of the laser pulse, and $\alpha_1$ is the linear absorption coefficient in material region 1. Due to Eq. (7) the solution of the problem is valid only within the pulse duration. However, according to Refs. [1,2] a solution can be written down easily for the cooling cycle after the laser pulse by adding a second solution using a negative source term for $t_p \leqslant t \leqslant \infty$ with equal strength $S$. Both solutions cover the full-time domain but do not consider thermal radiation losses $\sim T^4$ since the free emission of electromagnetic waves is not presumed for the laser heated internal interface between regions 1 and 2.

For solving the heat equation different techniques can be exploited as established in [2]. As demonstrated, the application of the Laplace transformation is a convenient way for solving the heat equation in different configurations of the source term and various boundary conditions [2,20].

Applying Laplace transformation the subsidiary equations of Eqs. (2) and (3) are

$$\frac{\partial^2 V_1}{\partial x_1^2} - q_1^2 \cdot \frac{\partial V_1}{\partial t} = \frac{I_V \cdot \alpha_1}{k_1 \cdot s} \cdot \mathrm{e}^{-\alpha_1 \cdot x_1} \tag{8}$$

and

$$\frac{\partial^2 V_2}{\partial x_2^2} - q_2^2 \cdot \frac{\partial V_2}{\partial t} = 0 \tag{9}$$

with

$$q_1^2 = \frac{s}{D_1} \quad \text{and} \quad q_2^2 = \frac{s}{D_2}. \tag{10}$$

The Laplace transformations of the initial and boundary conditions (6) and (7) give

$$V_1(x_1,0) = V_2(x_2,0) = 0 \tag{11}$$

and

$$k_1 \cdot \frac{\partial V_1(0,s)}{\partial x_1} = k_2 \cdot \frac{\partial V_2(0,s)}{\partial x_2}, \tag{12}$$

respectively. The principal solutions of the subsidiary equations (8) and (9) are

$$V_1 = C_1 \cdot \mathrm{e}^{-q_1 \cdot x_1} + \frac{I_V \cdot \alpha_1}{k_1 \cdot s \cdot (\alpha_1^2 - q_1^2)} \cdot \mathrm{e}^{-\alpha_1 \cdot x_1} \tag{13}$$

and

$$V_2 = C_2 \cdot \mathrm{e}^{-q_2 \cdot x_2}. \tag{14}$$

The unknown coefficients $C_1$ and $C_2$ are found from the initial and the boundary conditions given in Eqs. (11) and (12). The solution of the subsidiary equation for the non-absorbing solid material (region 2) heated indirectly by the laser-heated liquid is

$$V_2 = \frac{\sqrt{D_1}\cdot I_V}{k_2\cdot\sqrt{D_1}+k_1\cdot\sqrt{D_2}}\cdot\left[\begin{array}{l}\frac{1}{D_1\cdot\alpha_1^2}\cdot\frac{e^{-q_2\cdot x_2}}{q_2}+\frac{e^{-q_2\cdot x_2}}{s\cdot q_2}\\ -\frac{\sqrt{D_2}}{\sqrt{D_1}\cdot\alpha_1}\cdot\frac{e^{-q_2\cdot x_2}}{s}-\frac{1}{D_1\cdot\alpha_1^2}\cdot\frac{e^{-q_2\cdot x_2}}{q_2+\alpha_1\cdot\sqrt{D_1/D_2}}\end{array}\right] \tag{15}$$

after calculating the partial fractions and some simplifications. Thanks to the partial fraction decomposition the temperature in the solid material (region 2) can be calculated using tables of Laplace transforms [2].

Accordingly, the temperature $T_2$ is given by

$$T_2 = \frac{\sqrt{D_1}}{k_2\cdot\sqrt{D_1}+k_1\cdot\sqrt{D_2}}\cdot I_V\cdot\left[\begin{array}{l}\frac{1}{D_1\cdot\alpha_1^2}\cdot\sqrt{\frac{D_2}{\pi\cdot t}}\cdot e^{-\left(\frac{x_2^2}{4D_2\cdot t}\right)}+\mathrm{ierfc}\left(\frac{x_2}{2\cdot\sqrt{D_2\cdot t}}\right)-\frac{\sqrt{D_2}}{\sqrt{D_1}\cdot\alpha_1}\cdot\mathrm{erfc}\left(\frac{x_2}{2\cdot\sqrt{D_2\cdot t}}\right)-\frac{1}{D_1\cdot\alpha_1^2}\cdot\left(\sqrt{\frac{D_2}{\pi\cdot t}}\cdot e^{-\left(\frac{x_2^2}{4D_2\cdot t}\right)}\right.\\ \left.-\alpha_1\cdot\sqrt{D_1\cdot D_2}\cdot e^{\alpha_1\cdot\sqrt{D_1/D_2}\cdot x_2+\alpha_1^2\cdot D_1\cdot t}\cdot\mathrm{erfc}\left(\frac{x_2}{2\cdot\sqrt{D_2\cdot t}}+\alpha_1\cdot\sqrt{D_1\cdot t}\right)\right)\end{array}\right]. \tag{16}$$

The solution of Eq. (2) for region 1 where the laser beam is absorbed is given in Appendix A.

The temperature near the interface of an absorbing liquid and a transparent solid having the material properties listed in Table 1 is shown in Fig. 2 at the end of a single laser pulse of a length of 20 ns with the power density of $2.5\times10^{11}$ W m$^{-2}$. Due to the laser beam absorption in the liquid an almost exponential decay of the temperature is visible except for the near-interface region where the temperature drops down rapidly. The maximum temperature is not observed at the materials' interface where the laser beam has the highest power density but occurs at a distance in the liquid similar to the thermal diffusion length.

increases with the irradiance [1]. Therefore, the consideration of an additional heat source at the interface of the two materials is of essential practical importance.

The absorption at surfaces and interfaces is considered in the boundary condition. Therefore, Eq. (6) must be extended by a source term that accounts for the laser absorption as:

$$k_1\cdot\frac{\partial T_1(0,t)}{\partial x_1} = k_2\cdot\frac{\partial T_2(0,t)}{\partial x_2} - I_I. \tag{17}$$

Due to the interface absorption the laser intensity at the liquid surface $I_V$ is lower according to $I_V = I_L - I_I$.

Using this extended boundary condition of Eq. (17) and performing the whole procedure of Laplace transformation, solving the differential equation, and applying inverse Laplace transformation this problem has been solved in a similar way. In consequence, an additional term has to be added to the result of a non-absorbing interface given in Eq. (16). This additional term corresponds to the result of a pure surface heating but is weighted by the thermal coefficients of the adjoining materials. In other words, the superposition of temperature fields of independent sources, namely the interface absorption and the volume absorption, results in the simple addition of the mentioned term. The solution for the liquid (see Appendix B) is similar to the solid materials region, but differs in an additional term describing the interface source term.

$$T_2 = \frac{\sqrt{D_1}}{k_2\cdot\sqrt{D_1}+k_1\cdot\sqrt{D_2}}\cdot\left\{\begin{array}{l}I_V\cdot\left[\begin{array}{l}\frac{1}{D_1\cdot\alpha_1^2}\cdot\sqrt{\frac{D_2}{\pi\cdot t}}\cdot e^{-\left(\frac{x_2^2}{4D_2\cdot t}\right)}+\mathrm{ierfc}\left(\frac{x_2}{2\cdot\sqrt{D_2\cdot t}}\right)-\frac{\sqrt{D_2}}{\sqrt{D_1}\cdot\alpha_1}\cdot\mathrm{erfc}\left(\frac{x_2}{2\cdot\sqrt{D_2\cdot t}}\right)\\ -\frac{1}{D_1\cdot\alpha_1^2}\cdot\left(\sqrt{\frac{D_2}{\pi\cdot t}}\cdot e^{-\left(\frac{x_2^2}{4D_2\cdot t}\right)}-\alpha_1\cdot\sqrt{D_1\cdot D_2}\cdot e^{\alpha_1\cdot\sqrt{D_1/D_2}\cdot x_2+\alpha_1^2\cdot D_1\cdot t}\cdot\mathrm{erfc}\left(\frac{x_2}{2\cdot\sqrt{D_2\cdot t}}+\alpha_1\cdot\sqrt{D_1\cdot t}\right)\right)\end{array}\right]\\ +I_I\cdot\mathrm{ierfc}\left(\frac{x_2}{2\cdot\sqrt{D_2\cdot t}}\right)\end{array}\right\}. \tag{18}$$

### 2.3. Consideration of an additional absorption at the materials' interface

As known from different fields of physics, surfaces and interfaces are specific regions with different properties in relation to bulk materials. Especially structural defects appear. Moreover, the surface can be modified by additional substances such as contaminants that can change its properties, too. Such processes are known as adsorption that often occurs at solid–liquid interfaces. Both the intrinsic defects of the material interface and the "contaminants" can increase the absorption of light, i.e. of the laser radiation. Such a surface-enhanced absorption is regularly observed in laser processing. Moreover, at prolonged laser irradiation defects can be generated in materials, especially near the surface. Such laser-induced defects cause the well-known incubation effect in laser-assisted processes, i.e. the laser-initiated effect

Often the temperature at specific points is of particular interest especially for practical aspects. Therefore, the interface temperature ($x = 0$) was calculated from $T_2$ using Eq. (18) and is given by

$$T_I = \frac{\sqrt{D_1}}{k_2\cdot\sqrt{D_1}+k_1\cdot\sqrt{D_2}}\cdot\left\{I_V\cdot\left[\frac{L_{T_2}}{\sqrt{\pi}}+\frac{1}{\alpha_1}\cdot\sqrt{\frac{D_2}{D_1}}\cdot\left(e^{\left(\frac{\alpha_1\cdot L_{T_1}}{2}\right)^2}\cdot\mathrm{erfc}\left(\frac{\alpha_1\cdot L_{T_1}}{2}\right)-1\right)\right]+I_I\cdot\frac{L_{T_2}}{\sqrt{\pi}}\right\} \tag{19}$$

with $L_{T_n} = 2\cdot\sqrt{D_n\cdot t}$.

With increasing absorption of the liquid the interface temperature approaches the value of solely interface absorption which causes maximum interface temperatures. Consequently, high interface temperatures are achieved with highly absorbing liquids.

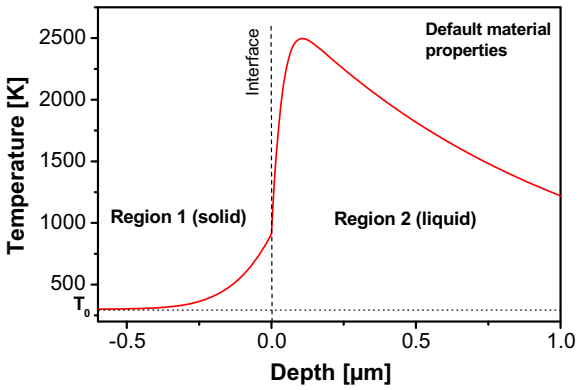


**Fig. 2.** Temperature across a laser-heated materials interface consisting of a transparent material and an absorbing material ($I_V = 2.5 \times 10^{11}$ W m$^{-2}$, $t_p = 20$ ns, default material).

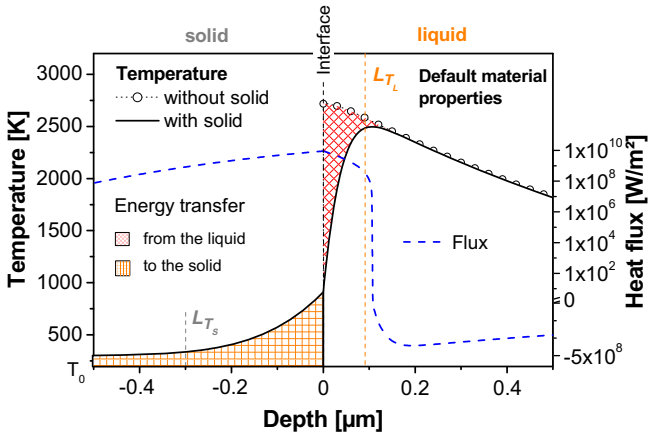


**Fig. 3.** Temperature and heat flux across the solid–liquid interface at $t = t_p$. Additionally, the temperature without a solid material is shown. The thermal diffusion lengths in both materials ($L_{T_S}; L_{T_L}$) are marked. The hatched areas illustrate the energy transferred by the heat flow.

For high absorption values, i.e. $\alpha_1 \cdot L_{T_1} \ll 1$, Eq. (19) can be approximated by

$$T_I = \frac{\sqrt{D_1}}{k_2 \cdot \sqrt{D_1} + k_1 \cdot \sqrt{D_2}} \cdot \left\{ I_V \cdot \frac{\alpha_1}{4} \cdot L_{T_1} \cdot L_{T_2} + I_I \cdot \frac{L_{T_2}}{\sqrt{\pi}} \right\}. \quad (20)$$

The temperature across a materials interface with a partial absorption of the laser radiation by the interface in comparison to the temperature distribution without the interface absorption is shown in Fig. 3. The substantial influence of interface absorption on the maximum temperature and its spatial dependence are clearly depicted.

## 3. Discussion

The achieved temperature fields across the materials interface are analyzed concerning the influence of material parameters and the laser energy deposition. The basic parameters were chosen to represent materials properties of typical solid–liquid interfaces. The used material parameters are listed in Table 1 but can be obtained in general from data pools [22,23] for different wavelengths.

The achieved solutions are valid for time scales larger than the relaxation time of excited states into the phonon system so that the source term of Eq. (2) can be described by Beer's law Eq. (7). The primary energy deposition in the case of high energy laser pulses ($I_L > 10^9$ W/cm$^2$) that can be easily exceeded by applying focused ultrashort laser pulses ($t_p \sim 10^{-15}$–$10^{-12}$ s) can, however, differ from the linear absorption provided by Beer's law and must be described by multi-photon absorption and/or avalanche processes. Also, specific material characteristics, e.g. light scattering into the material, can result in a different energy deposition as the optical path is modified, i.e. extended. Resonances in globular composites may also influence the light absorption. In these cases either refined solutions of the found results are required or averaged values of the absorption (absorption coefficient or penetration depth) can be used as a first approximation. Also for the case of weak absorbing solids (region 2) the given solution is a good approximation with the condition $\alpha_1 \gg \alpha_2$ and the consideration of the absorption $\alpha_2$ in region 2 for calculation $I_L$.

The analytical solution is useful for ns-laser irradiation of materials interfaces as the lower limit is given by the electron–phonon coupling time constant ($t \sim 10^{-11}$ s) and the upper limit ($t \sim 10^{-3}$ s) results from the transfer of the solution to the special case of pure interface absorption. However, this time domain covers exactly the pulse length of typically used pulsed laser sources and therefore meets the requirements of practical temperature calculations.

If not specified otherwise the following parameters were used for calculations; the laser source has a pulse length of 20 ns and a fluence $F$ of $5 \times 10^4$ J m$^{-2}$, the initial temperature was set to 300 K and the default material parameters of Table 1 were applied.

### 3.1. Relevance of interface absorption for materials processing

The temperature and the heat flux across the solid–liquid interface are shown in Fig. 3 for typical processing parameters and weakly absorbing liquids ($L_{T_L} \ll L_{O_L}$). Due to the rather low absorption of the liquid the heated material depth is much higher in the liquid than it is in the solid material which is heated by thermal conduction only.

Therefore, the heated solid depth is similar the thermal diffusion length that is additionally shown in Fig. 3. Further, the temperature in the liquid phase without an adjacent solid surface is shown. A remarkable difference in the liquid temperatures near the interface with and without the solid material is depicted in Fig. 3. It can be attributed to the "cooling" of the laser-heated liquid by the thermal flow to the solid material. Due to this heat transport, the maximal temperature is inside the liquid absorber with a distance to the interface that is approximately equal the thermal diffusion length of the liquid.

The thermal flow across the interface (also depicted in Fig. 3) shows clearly that the heat flow from the laser-heated liquid to the solid is limited by the thermal diffusion length of the liquid. The heat flow goes into reverse (negative values) at larger distances from the interface. The heat flux through the interface is about 1.5 orders of magnitude less than the power density of the laser beam of $2.5 \times 10^{11}$ W m$^{-2}$. Therefore, a limitation of the overall transferred energy can be expected. The energy that is transferred from the liquid to the heated solid is marked in the figure and can be calculated from the difference in the laser-induced temperatures achieved with and without the solid (see Fig. 3). Because the heated liquid volume is equivalent the optical penetration depth that is much larger than the thermal diffusion length of the liquid only 2.5% of the laser energy were utilized for solid heating at a liquid absorption coefficient of $\alpha_L = 1 \times 10^6$ m$^{-1}$.

Fig. 4 shows the percentage of the laser energy utilized for heating the solid material in dependence of the absorption coefficient of the liquid for two different interface absorption values. At low absorption coefficients where the optical penetration depth is much larger than the thermal diffusion length only low laser energy is transferred to the solid. However, with the reduction of the optical penetration depth the energy transferred to the solid increases and finally reaches the limit given by pure interface absorption. For optimal utilization of the laser energy a partial laser absorption at the interface (e.g. 30% as shown in the figure) causes a much higher energy transfer to the solid and consequently higher temperatures compared to solely utilization of high absorbing liquids.

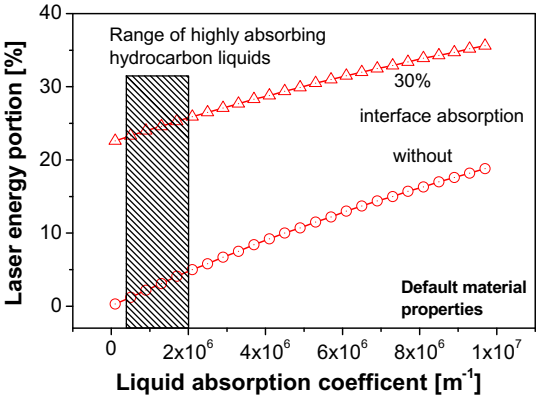


**Fig. 4.** Portion of the laser energy utilized for solid heating.

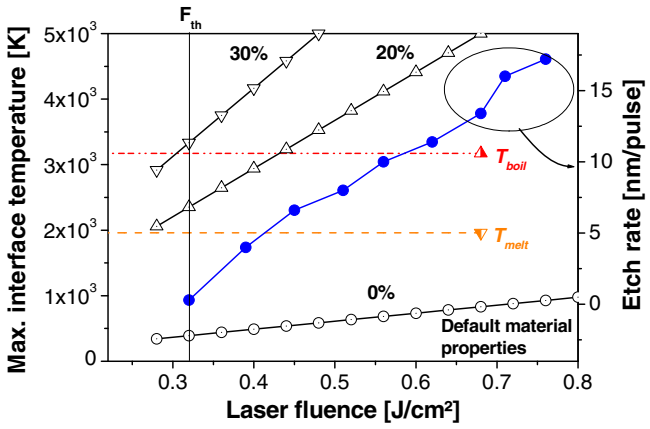


**Fig. 6.** Etch rate of fused silica at LIBWE and maximum interface temperatures caused by laser irradiation ($\lambda = 248$ nm, $t_p \sim 25$ ns) for three different interface absorption values (0%, 20%, 30%) in dependence on the applied laser fluence. The melting and vaporization temperatures of fused silica are shown in addition.

### *3.2. Comparison with numerical calculations using temperature-dependent material parameters*

As known the material properties depend on various parameters, e.g. the temperature. For the evaluation of the influence of real material parameters on the temperature the analytical results were compared to numerical values considering the temperature dependence of both the specific heat and the thermal conductivity of the solid whereas the liquid properties were kept constant.

In Fig. 5 the temperatures across the interface calculated analytically and numerically with constant coefficients (values at $T_0$ are used) are compared with the temperatures achieved with temperature-dependent material properties. The analytically calculated temperatures agree with the numerical ones very well as shown in Fig. 5. The slightly lower temperatures resulting from the numerical calculations using temperature-dependent coefficients are the consequence of the rise of the specific heat and the thermal conductivity with the temperature. Nevertheless, the approximation of the analytical solution to the numerical results can basically be improved when the coefficients of an average temperature are used.

### *3.3. Discussion of experimental results of LIBWE*

As already mentioned laser beam absorption at material interfaces is used for LIBWE which allows high-quality etching of transparent materials, e.g. fused silica, with UV laser radiation ($\lambda = 248$ nm, $t_p \sim 25$ ns) [14,17–19]. The mechanism of materials etching results from highly dynamic processes at the liquid–solid interface that are caused by the absorption of the laser beam and the subsequent materials heating near the interface. In Fig. 6 the etch rate is shown in comparison to the maximum interface temperature upon laser irradiation. Clearly, the etching threshold ($F_{th}$) as well as an approximately linear increase of the etch rate are characteristics of the etching process. However, the fused silica surface temperature does not reach the melting temperature at the threshold without partially interface absorption (0%) so that materials etching cannot be expected. In fact, absorption measurements at the laser wavelength show a significant surface absorption of the laser-etched fused silica that amounts about 32% at the etching threshold [21]. The temperatures calculated by the model considering both liquid and interface absorption (30%) exceed the vaporization temperature of fused silica by far as shown in the figure. Moreover, the linear growth of the etch rate is in accordance with the linear increase of the temperature with rising laser fluence. Therefore, it can be suggested that the etching process is determined by the explosive vaporization of the fused silica.

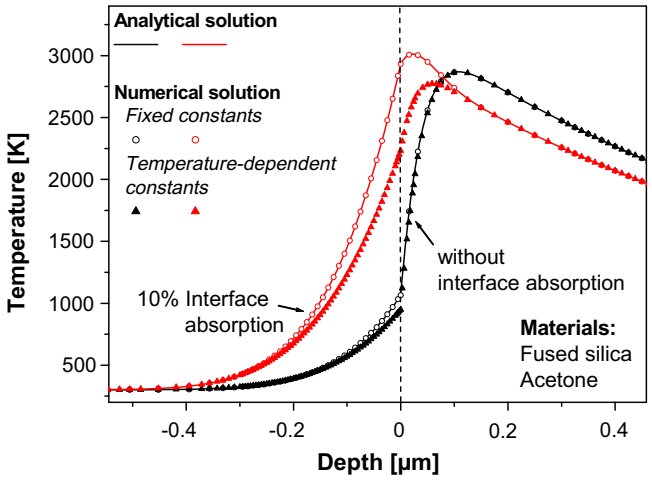


**Fig. 5.** Comparison of the analytical with the numerical results calculated using either constant (at $T_0$) or temperature-dependent coefficients.

## 4. Conclusions

An analytical solution of the heat conduction equation with constant coefficients has been developed for laser-irradiated material interfaces. The model considers the laser absorption in one material as well as at the interface. The achieved results in terms of temperature distribution, the thermal flow, and the energy efficiency for heating the solid interface partner show that the material properties, the distribution of the absorbed laser energy, and the pulse duration of the laser pulse have a major influence on the thermal processes. In order to achieve high interface or solid surface temperatures as well as efficient laser energy utilization sufficient interface absorption is required especially for good heat conducting solids. Although theoretically high interface temperatures can be achieved by high absorbing liquids the thermal resistance of the liquid limits the heat flow to the solid material, too. For technical applications the attained solution agrees sufficiently with numerical results which consider temperature-dependent material parameters. Finally, it allows the interpretation of experimental results as shown for the LIBWE process.

## Acknowledgements

The author is grateful to E. Salamatin for careful reading the manuscript and R. Böhme for the stimulating discussions.

## Appendix A

Solution of Eq. (2) for temperature calculations in the region 1 (liquid), which absorbs the laser radiation, without interface absorption.

$$T_1 = I_V \cdot \left\{ \begin{array}{l} \frac{e^{-(\alpha_1 \cdot x_1)}}{k_1 \cdot \alpha_1} \cdot \left(e^{(D_1 \cdot \alpha_1^2 \cdot t)} - 1\right) + \frac{\sqrt{D_2}}{k_2 \cdot \sqrt{D_1} + k_1 \cdot \sqrt{D_2}} \cdot \\ \left[ \begin{array}{l} \frac{1}{D_1 \cdot \alpha_1^2} \cdot \sqrt{\frac{D_1}{\pi \cdot t}} \cdot e^{-\left(\frac{x_1^2}{4 D_1 \cdot t}\right)} + \text{ierfc}\left(\frac{x_1}{2 \cdot \sqrt{D_1 \cdot t}}\right) - \frac{k_2 \cdot \sqrt{D_1}}{\alpha_1 \cdot k_1 \cdot \sqrt{D_2}} \cdot \text{erfc}\left(\frac{x_1}{2 \cdot \sqrt{D_1 \cdot t}}\right) \\ + \frac{1}{D_1 \cdot 2 \cdot \alpha_1^2} \cdot \left( \begin{array}{l} \left(\frac{k_2 \cdot \sqrt{D_1}}{k_1 \cdot \sqrt{D_2}} - 1\right) \cdot \left(\sqrt{\frac{D_1}{\pi \cdot t}} \cdot e^{-\left(\frac{x_1^2}{4 D_1 \cdot t}\right)} - \alpha_1 \cdot D_1 \cdot e^{\alpha_1 \cdot x_1 + \alpha_1^2 \cdot D_1 \cdot t} \cdot \text{erfc}\left(\frac{x_1}{2 \cdot \sqrt{D_1 \cdot t}} + \alpha_1 \cdot \sqrt{D_1 \cdot t}\right)\right) \\ + \left(\frac{k_2 \cdot \sqrt{D_1}}{k_1 \cdot \sqrt{D_2}} + 1\right) \cdot \left(\sqrt{\frac{D_1}{\pi \cdot t}} \cdot e^{-\left(\frac{x_1^2}{4 D_1 \cdot t}\right)} + \alpha_1 \cdot D_1 \cdot e^{-\alpha_1 \cdot x_1 + \alpha_1^2 \cdot D_1 \cdot t} \cdot \text{erfc}\left(\frac{x_1}{2 \cdot \sqrt{D_1 \cdot t}} - \alpha_1 \cdot \sqrt{D_1 \cdot t}\right)\right) \end{array} \right) \end{array} \right] \end{array} \right\}$$

with $I_V = I_0$.

## Appendix B

Solution of Eq. (2) for temperature calculations in the region 1 (liquid) with interface absorption.

$$T_1 = I_V \cdot \left\{ \begin{array}{l} \frac{e^{-(\alpha_1 \cdot x_1)}}{k_1 \cdot \alpha_1} \cdot \left(e^{(D_1 \cdot \alpha_1^2 \cdot t)} - 1\right) + \frac{\sqrt{D_2}}{k_2 \cdot \sqrt{D_1} + k_1 \cdot \sqrt{D_2}} \cdot \\ \left[ \begin{array}{l} \frac{1}{D_1 \cdot \alpha_1^2} \cdot \sqrt{\frac{D_1}{\pi \cdot t}} \cdot e^{-\left(\frac{x_1^2}{4 D_1 \cdot t}\right)} + \text{ierfc}\left(\frac{x_1}{2 \cdot \sqrt{D_1 \cdot t}}\right) - \frac{k_2 \cdot \sqrt{D_1}}{\alpha_1 \cdot k_1 \cdot \sqrt{D_2}} \cdot \text{erfc}\left(\frac{x_1}{2 \cdot \sqrt{D_1 \cdot t}}\right) \\ + \frac{1}{D_1 \cdot 2 \cdot \alpha_1^2} \cdot \left( \begin{array}{l} \left(\frac{k_2 \cdot \sqrt{D_1}}{k_1 \cdot \sqrt{D_2}} - 1\right) \cdot \left(\sqrt{\frac{D_1}{\pi \cdot t}} \cdot e^{-\left(\frac{x_1^2}{4 D_1 \cdot t}\right)} - \alpha_1 \cdot D_1 \cdot e^{\alpha_1 \cdot x_1 + \alpha_1^2 \cdot D_1 \cdot t} \cdot \text{erfc}\left(\frac{x_1}{2 \cdot \sqrt{D_1 \cdot t}} + \alpha_1 \cdot \sqrt{D_1 \cdot t}\right)\right) \\ + \left(\frac{k_2 \cdot \sqrt{D_1}}{k_1 \cdot \sqrt{D_2}} + 1\right) \cdot \left(\sqrt{\frac{D_1}{\pi \cdot t}} \cdot e^{-\left(\frac{x_1^2}{4 D_1 \cdot t}\right)} + \alpha_1 \cdot D_1 \cdot e^{-\alpha_1 \cdot x_1 + \alpha_1^2 \cdot D_1 \cdot t} \cdot \text{erfc}\left(\frac{x_1}{2 \cdot \sqrt{D_1 \cdot t}} - \alpha_1 \cdot \sqrt{D_1 \cdot t}\right)\right) \end{array} \right) \end{array} \right] \end{array} \right\}$$

with $I_V = I_0 - I_l$.

## References

[1] D. Bäuerle, Laser Processing and Chemistry, Springer, Berlin, 2000.
[2] H.S. Carslaw, J.C. Jaeger, Conduction of Heat in Solid, Oxford University Press, Oxford, 1959.
[3] J.F. Li, L. Li, F.H. Stott, A three-dimensional numerical model for a convection–diffusion phase change process during laser melting of ceramic materials, Int. J. Heat Mass Transfer 47 (25) (2004) 5523–5539.
[4] C. Schäfer, H.M. Urbassek, L.V. Zhigilei, Metal ablation by picosecond laser pulses: a hybrid simulation, Phys. Rev. B 66 (11) (2002) 1154041–1154048.
[5] J.K. Chen, D.Y. Tzou, J.E. Beraun, A semiclassical two-temperature model for ultrafast laser heating, Int. J. Heat Mass Transfer 49 (1–2) (2006) 307–316.
[6] S.I. Anisimov, B.l. Kapeliovich, T.L. Perelman, Electron-emission from surface of metals induced by ultrashort laser pulses, Zh. Eksp. Teor. Fiz. 66 (2) (1974) 776–781.
[7] R.J. Goldstein, E.R.G. Eckert, W.E. Ibele, S.V. Patankar, T.W. Simon, T.H. Kuehn, P.J. Strykowski, K.K. Tamma, J.V.R. Heberlein, J.H. Davidson, Heat transfer – a review of 2001 literature, Int. J. Heat Mass Transfer 46 (11) (2003) 1887–1992.
[8] L.X. Yang, X.F. Peng, B.X. Wang, Numerical modelling and experimental investigation on the characteristics of molten pool during laser processing, Int. J. Heat Mass Transfer 44 (23) (2001) 4465–4473.
[9] A. Kruusing, Underwater and water-assisted laser processing. Part 1 – General features, steam cleaning and shock processing, Opt. Laser Eng. 41 (2) (2004) 307–327.
[10] S.I. Dolgaev, A.V. Simakin, V.V. Voronov, G.A. Shafeev, F. Bozon-Verduraz, Nanoparticles produced by laser ablation of solids in liquid environment, Appl. Surf. Sci. 186 (1–4) (2002) 546–551.
[11] T. Sakka, K. Saito, Y.H. Ogata, Confinement effect of laser ablation plume in liquids probed by self-absorption of C-2 Swan band emission, J. Appl. Phys. 97 (1) (2005) 0149021–0149024.
[12] A. Dupont, P. Caminat, P. Bournot, J.P. Gauchon, Enhancement of material ablation using 248, 308, 532, 1064 nm laser pulse with a water film on the treated surface, J. Appl. Phys. 78 (3) (1995) 2022–2028.
[13] T. Tsuji, T. Kakita, M. Tsuji, Preparation of nano-size particles of silver with femtosecond laser ablation in water, Appl. Surf. Sci. 206 (1–4) (2003) 314–320.
[14] J. Wang, H. Niino, A. Yabe, One-step microfabrication of fused silica by laser ablation of an organic solution, Appl. Phys. A 68 (1) (1999) 111–113.
[15] H.S. Mavi, S. Prusty, M. Kumar, R. Kumar, A.K. Shulka, S. Rath, Formation of Si and Ge quantum structures by laser-induced etching, Phys. Status Solidi A 203 (10) (2006) 2444–2450.
[16] M. Mosbacher, V. Dobler, J. Boneberg, P. Leiderer, Universal threshold for the steam laser cleaning of submicron spherical particles from silicon, Appl. Phys. A 70 (6) (2000) 669–672.
[17] R. Böhme, A. Braun, K. Zimmer, Backside etching of UV-transparent materials at the interface to liquids, Appl. Surf. Sci. 186 (1–4) (2002) 276–281.
[18] B. Hopp, T. Smausz, N. Barna, C. Vass, Z. Antal, L. Kredics, D. Chrisey, Time-resolved study of absorbing film assisted laser induced forward transfer of *Trichoderma longibrachiatum* conidia, J. Phys. D 38 (6) (2005) 833–837.
[19] K. Zimmer, R. Böhme, D. Ruthe, B. Rauschenbach, Backside laser etching of fused silica using liquid gallium, Appl. Phys. A 84 (4) (2006) 455–458.
[20] G. Araya, G. Gutierrez, Analytical solution for a transient three-dimensional temperature distribution due to a moving laser beam, Int. J. Heat Mass Transfer 49 (21–22) (2006) 4124–4131.
[21] R. Böhme, Laser-induced backside wet etching of glasses and crystals, Ph.D. Thesis, Martin-Luther-Universität Halle-Wittenberg, Halle, 2007. Available from: http://sundoc.bibliothek.uni-halle.de/diss-online/07/07H107/index.htm.
[22] D.N. Nikogosyan, Properties of Optical and Laser-Related Materials – A Handbook, Wiley, New York, 1997.
[23] http://www.mt-berlin.com/frames_cryst/descriptions/sapphire.htm.